

SUPPLEMENTARY METHODS

CONTENTS:

1. BASIC sRNA AND TF MODELS
2. EXTENDED sRNA MODEL
3. COMMENTS ON sRNA DEGRADATION RATES
4. TIME LAG
5. SUPPLEMENTARY REFERENCES
6. SUPPLEMENTARY FIGURE AND TABLE LEGENDS

1. BASIC sRNA AND TF MODELS

Our basic model, which treats duplex formation as a single bimolecular reaction step, is very similar to that previously described (4-7). The equations are:

$$\frac{d[\text{sRNA}]}{dt} = \alpha_S - k[\text{sRNA}][\text{mRNA}] - \beta_S[\text{sRNA}], \quad [\text{S1}]$$

$$\frac{d[\text{mRNA}]}{dt} = \alpha_M - k[\text{sRNA}][\text{mRNA}] - \beta_M[\text{mRNA}], \quad [\text{S2}]$$

$$\frac{d[\text{duplex}]}{dt} = k[\text{sRNA}][\text{mRNA}] - \beta_D[\text{duplex}], \text{ and} \quad [\text{S3}]$$

$$\frac{d[\text{P}]}{dt} = \alpha_P[\text{mRNA}] - \beta_P[\text{P}]. \quad [\text{S4a}]$$

[sRNA], [mRNA], [duplex] and [P] are the concentrations of the sRNA, target mRNA, duplex and target protein respectively [units: nM]. α_S and α_M are the production rates for the sRNA and mRNA [units: $\text{nM}\cdot\text{min}^{-1}$] and α_P is the target protein production rate [units: $\text{protein nM}\cdot(\text{mRNA nM})^{-1}\cdot\text{min}^{-1}$]. β_S , β_M , β_D and β_P are the degradation rate constants for the sRNA, target mRNA, duplex and target protein respectively [units: min^{-1}]. k is the rate constant for duplex annealing [units: $\text{nM}^{-1}\cdot\text{min}^{-1}$]. Parameter values are provided in the **Materials and Methods**. The model assumes that duplex dissociation is negligible and that each sRNA silences or activates only one target mRNA (we are unaware of physiological evidence to the contrary). Symbols and terms defined by Levine and colleagues (7) are used where applicable. sRNA

activation of gene translation was modeled with the same set of equations except duplex mRNA is translated rather than the free mRNA therefore **Eq. S4a** is replaced by

$$\frac{d[P]}{dt} = \alpha_D [\text{duplex}] - \beta_P [P], \quad [\text{S4b}]$$

where α_D is the rate of protein production from the duplex [units: protein nM·(mRNA nM)⁻¹·min⁻¹]. For simplicity we assume $\alpha_D = \alpha_P$.

Solving the above dynamic equations at steady state yielded the analytic solutions for the target protein ([P*]) and target mRNA ([mRNA*]) concentrations. For silencing sRNAs,

$$[P^*] = \frac{\alpha_P}{\beta_P} [mRNA^*],$$

$$\text{where } [mRNA^*] = \frac{1}{2\beta_M} \left[\left(\alpha_M - \alpha_S - \frac{\beta_M \beta_S}{k} \right) + \sqrt{\left(\alpha_M - \alpha_S - \frac{\beta_M \beta_S}{k} \right)^2 + \frac{4\alpha_M \beta_M \beta_S}{k}} \right]. \quad [\text{S5}]$$

[mRNA*] is the steady state target mRNA concentration and its derivation has been reported (7). For activating sRNAs,

$$[P^*] = \frac{\alpha_D}{\beta_P} [\text{duplex}^*] = \frac{\alpha_D}{\beta_P} \left(\frac{\alpha_S k [mRNA^*]}{\beta_D k [mRNA^*] + \beta_S \beta_D} \right), \quad [\text{S6}]$$

where [duplex*] is the steady state duplex concentration.

The TF circuits were modeled using a set of dynamic equations with the repression and the activation of transcription described with standard Hill functions (13). The set of dynamic equations used to model TF repression are:

$$\frac{d[\text{TF mRNA}]}{dt} = \alpha_{\text{TFM}} - \beta_{\text{TFM}} [\text{TF mRNA}], \quad [\text{S7}]$$

$$\frac{d[\text{TF}]}{dt} = \alpha_{\text{TFP}} [\text{TFmRNA}] - \beta_{\text{TFP}} [\text{TF}], \quad [\text{S8}]$$

$$\frac{d[\text{mRNA}]}{dt} = \frac{\alpha_M}{1 + ([\text{TF}] / K_D)^n} - \beta_M [\text{mRNA}], \quad [\text{S9a}]$$

$$\frac{d[P]}{dt} = \alpha_P [\text{mRNA}] - \beta_P [P]. \quad [\text{S10}]$$

[TF mRNA] and [TF] are the concentrations of the TF repressor mRNA and protein respectively. α_{TFM} is the TF mRNA transcription rate [units: nM·min⁻¹] and α_{TFP} is the TF production rate [units: protein nM·(mRNA nM)⁻¹·min⁻¹]. β_{TFM} and β_{TFP} are the degradation rate constants for TF mRNA and TF respectively [units: min⁻¹]. K_D is the constant [units: nM] that determines the TF concentration resulting in half-maximal transcription of the target gene and n is the Hill coefficient [unitless] which specifies the amount of cooperativity. All other rate constants are the same as for the sRNA circuits and the parameter values are provided in the **Materials and Methods**. Note: **Eq. S4a** and **Eq. S10** are the same for sRNA silencing and TF repression. To model the TF activator, **Eq. S9a** is replaced by

$$\frac{d[\text{mRNA}]}{dt} = \frac{\alpha_M [\text{TF}]^n}{K_D^n + [\text{TF}]^n} - \beta_M [\text{mRNA}]. \quad [\text{S9b}]$$

For simplicity, the parameter values for the repressor and activator are the same but this does not need to be the case.

The steady state solutions to the dynamic equations for the TF circuits are:

$$[P^*] = \frac{\alpha_P}{\beta_P} [\text{mRNA}^*], \text{ where}$$

$$[\text{mRNA}^*] = \frac{\alpha_M}{\beta_M} \left[1 + \left(\frac{\alpha_{TFM} \alpha_{TFP}}{\beta_{TFM} \beta_{TFP} K_D} \right)^n \right]^{-1} \text{ for the TF repressor and} \quad [\text{S11}]$$

$$[\text{mRNA}^*] = \frac{\alpha_M}{\beta_M} \left(1 - \left[1 + \left(\frac{\alpha_{TFM} \alpha_{TFP}}{\beta_{TFM} \beta_{TFP} K_D} \right)^n \right]^{-1} \right) \text{ for the TF activator.} \quad [\text{S12}]$$

2. EXTENDED sRNA MODEL

The extended sRNA model includes the role of Hfq in mediating duplex formation as shown in **Supplementary Figure S1A**. We have previously described a similar model (26) but in this study the model does not include competing sRNAs and target mRNAs from other pathways and there are different degradation rate constants for the different species. The sRNA binds first to Hfq followed by the target mRNA or the target mRNA binds to Hfq followed by the sRNA resulting in a ternary Hfq complex. We

assume that for each sRNA-target mRNA pair, one face of the Hfq hexamer is specific for the sRNA and the other is specific for its cognate target mRNA (*i.e.* ternary Hfq complexes with two sRNAs or two target mRNAs do not occur) (1). The sRNA and target mRNA in the ternary complex can anneal resulting in a stable sRNA-target mRNA duplex that is released. There is evidence that the duplex may not always be fully annealed before release (53) but this does not affect the model. Once the duplex forms we assume it does not significantly disassemble or re-bind free Hfq. Other than duplex formation and release all binding reactions are treated as reversible.

The set of differential equations used to describe the system are:

$$\frac{d[\text{sRNA}]}{dt} = \alpha_S + k_{-S}[\text{SH}] + k_{-\text{STH}}[\text{SHT}] - k_S[\text{sRNA}][\text{Hfq}] - k_{\text{STH}}[\text{sRNA}][\text{TH}] - \beta_S[\text{sRNA}] \quad [\text{S13}]$$

$$\frac{d[\text{mRNA}]}{dt} = \alpha_M + k_{-T}[\text{TH}] + k_{-\text{TSH}}[\text{SHT}] - k_T[\text{mRNA}][\text{Hfq}] - k_{\text{TSH}}[\text{mRNA}][\text{SH}] - \beta_M[\text{mRNA}] \quad [\text{S14}]$$

$$\begin{aligned} \frac{d[\text{Hfq}]}{dt} = & \alpha_H + k_{-S}[\text{SH}] + k_{-T}[\text{TH}] + k_{\text{DUP}}[\text{SHT}] + \beta_{\text{SH}}[\text{SH}] + \beta_{\text{TH}}[\text{TH}] \\ & \dots + \beta_{\text{SHT}}[\text{SHT}] - k_S[\text{sRNA}][\text{Hfq}] - k_T[\text{mRNA}][\text{Hfq}] - \beta_H[\text{Hfq}] \end{aligned} \quad [\text{S15}]$$

$$\frac{d[\text{SH}]}{dt} = k_S[\text{sRNA}][\text{Hfq}] + k_{-\text{TSH}}[\text{SHT}] - k_{-S}[\text{SH}] - k_{\text{TSH}}[\text{mRNA}][\text{SH}] - (\beta_{\text{SH}} + \beta_H)[\text{SH}] \quad [\text{S16}]$$

$$\frac{d[\text{TH}]}{dt} = k_T[\text{mRNA}][\text{Hfq}] + k_{-\text{STH}}[\text{SHT}] - k_{-T}[\text{TH}] - k_{\text{STH}}[\text{sRNA}][\text{TH}] - (\beta_{\text{TH}} + \beta_H)[\text{TH}] \quad [\text{S17}]$$

$$\frac{d[\text{SHT}]}{dt} = k_{\text{STH}}[\text{sRNA}][\text{TH}] + k_{\text{TSH}}[\text{mRNA}][\text{SH}] - (k_{-\text{STH}} + k_{-\text{TSH}} + k_{\text{DUP}} + \beta_{\text{SHT}} + \beta_H)[\text{SHT}] \quad [\text{S18}]$$

$$\frac{d[\text{duplex}]}{dt} = k_{\text{DUP}}[\text{SHT}] - \beta_{\text{D}}[\text{duplex}] \quad [\text{S19}]$$

[Hfq], [SH], [TH] and [SHT] are the concentrations of Hfq protein, sRNA-Hfq complex, target mRNA-Hfq complex, and sRNA-Hfq-target mRNA complex respectively. k_S , k_T , k_{STH} and k_{TSH} are the RNA binding rate constants and all were assigned a value of $1 \text{ nM}^{-1} \cdot \text{min}^{-1}$ unless otherwise stated (**Supplementary Figure S1A**). k_{-S} , k_{-T} , $k_{-\text{STH}}$ and $k_{-\text{TSH}}$ are the RNA dissociation rate constants and they were all assigned the same value of 0.1 min^{-1} unless otherwise stated (these values include the relatively small contribution that the dilution associated with cell growth has on their removal) (**Supplementary Figure S1A**). k_{DUP} is the rate constant for duplex annealing and release from the ternary complex and it was assigned a value

of 1 min^{-1} . α_H is the Hfq production rate which was $0.3 \text{ nM}\cdot\text{min}^{-1}$ unless otherwise stated and β_H is the Hfq degradation rate constant. The steady state Hfq concentration, which is equal to α_H/β_H , is generally thought to be relatively high *in vivo*. However, in our model we have a relatively low Hfq concentration because there are no competing sRNAs and target mRNAs to sequester the Hfq and reduce the free fraction as occurs *in vivo* (26). It is assumed that Hfq is only lost via the dilution associated with cell growth (*i.e.* $\beta_H = 0.03 \text{ min}^{-1}$ which is the same value as β_P above). β_{SH} , β_{TH} and β_{SHT} are the constants for the active degradation of sRNAs and TF mRNAs while bound to Hfq in SH, TH and SHT complexes. Note these constants differ from the β_S and β_M degradation rate constants which include active degradation plus the effect of dilution.

For sRNA silencers, the differential equation for the target protein concentration is

$$\frac{d[P]}{dt} = \alpha_P ([\text{mRNA}] + [\text{TH}] + [\text{SHT}]) - \beta_P [P], \quad [\text{S20a}]$$

which assumes that any form of the target mRNA that is not within a duplex is translated. This is consistent with experiments that have shown that target protein concentrations are not altered by the presence of Hfq (20) which indicates the mRNA and TH are translated at the same rates. It is possible that the target mRNAs within SHT ternary complexes are translated at a different rate however these complexes are likely to be a small fraction of the total target mRNA and thus any difference in their translation rate will have a minor effect on the target protein concentration. For sRNA activators, the differential equation for the target protein concentration is

$$\frac{d[P]}{dt} = \alpha_D [\text{duplex}] - \beta_P [P]. \quad [\text{S20b}]$$

3. COMMENTS ON sRNA DEGRADATION RATES

The degradation rate of sRNAs varies widely. A relatively short half-life of 2-5 min has been reported for DsrA, depending on the temperature and isoform (54) and 7-8 min for RprA (55). OxyS and GcvB have been shown to have intermediate half-lives of around 15 min (38,56). Other sRNAs such as Spot 42 and RyhB have half-lives $>30 \text{ min}$ (57,58). Furthermore, these half-lives are very dependent on conditions, particularly the availability of Hfq. For example, in the absence of Hfq the half-lives of Spot 42 and RyhB

decrease from >30 min to <2 min (57,58). Similarly, the half-life of GcvB decreases from ~15 min to 5 min in the absence of Hfq (56).

Due to the variation in sRNA degradation rates and their dependence on Hfq availability, which in turn depends also on the concentrations of all the target mRNAs and sRNAs in the cell that compete for a limited amount of Hfq (20,37), we simply assigned an average sRNA degradation rate constant that was equivalent to the average mRNA half-life (5 min). sRNAs that have longer lifetimes may have free concentrations that are up to 4 to 5 times greater than modeled. However the increased sRNA concentration will not have much impact on the response curves because most of the sRNAs will be in the form of duplexes. To demonstrate this we re-simulated sRNA silencing and sRNA activation in the basic model with sRNAs having half-lives of 21 min instead of 5 min ($\beta_s = 0.03 \text{ min}^{-1}$ versus 0.14 min^{-1}); the change in the sRNA degradation rates had minimal effect on the response curves (**Supplementary Figure S5**). While the longer half-lives of some sRNAs would have minimal effect on the response curves it is possible they may affect the dynamics. Longer half-lives would mean the clearance rate of excess sRNAs would be lower and therefore the time delay in turning off their activity could be greater. This effect would likely be offset to some extent by the fact that high concentrations of sRNAs are harder to achieve than for TFs (due to the lack of amplification that occurs with translation and their clearance through duplex formation) and because the response curve for sRNAs is typically linear.

4. TIME LAG

The models do not take into account the difference in the time required to produce the first sRNA and first TF protein. However this time lag is likely to be very small compared to the time scales needed to produce a significant change in target protein concentration. Assume the average lengths of a sRNA gene and TF gene are 100 and 1000 nucleotides respectively then the difference in the amount of time needed to transcribe these genes will be 900 nucleotides divided by the average transcription rate (42 nucleotides/s) (43). Therefore the TF mRNA takes ~ 20s longer to be transcribed. Translation of the mRNA occurs as the TF mRNA is being transcribed and the ribosomes progress at a rate that is equivalent to the RNA polymerase (59,60) therefore there is no need to factor additional time for

translation. Consequently the first TF is generated at approximately the same time as transcription of the first TF mRNA is completed. That is, the first TF will be produced ~20s after the first sRNA. There are no further delays after the first sRNA and TF mRNA are created and all subsequent sRNAs and TF mRNAs are generated at rates determined by the rates of transcriptional initiation and transcription, which will be approximately the same for sRNA and TF circuits if their promoters are approximately the same strength.

5. SUPPLEMENTARY REFERENCES

1. Vogel, J. and Luisi, B.F. (2011) Hfq and its constellation of RNA. *Nat Rev Microbiol*, **9**, 578-589.
4. Mehta, P., Goyal, S. and Wingreen, N.S. (2008) A quantitative comparison of sRNA-based and protein-based gene regulation. *Mol Syst Biol*, **4**, 221.
5. Shimoni, Y., Friedlander, G., Hetzroni, G., Niv, G., Altuvia, S., Biham, O. and Margalit, H. (2007) Regulation of gene expression by small non-coding RNAs: a quantitative view. *Mol Syst Biol*, **3**, 138.
6. Legewie, S., Dienst, D., Wilde, A., Herzog, H. and Axmann, I.M. (2008) Small RNAs establish delays and temporal thresholds in gene expression. *Biophys J*, **95**, 3232-3238.
7. Levine, E., Zhang, Z., Kuhlman, T. and Hwa, T. (2007) Quantitative characteristics of gene regulation by small RNA. *PLoS Biol*, **5**, e229.
13. Alon, U. (2007) *An Introduction to Systems Biology: Design Principles of Biological Circuits*. Chapman and Hall/CRC, Boca Raton, FL.
20. Hussein, R. and Lim, H.N. (2010) Disruption of small RNA signaling caused by competition for Hfq. *Proc Natl Acad Sci U S A*, **108**, 1110-1115.
21. Lutz, R., Lozinski, T., Ellinger, T. and Bujard, H. (2001) Dissecting the functional program of Escherichia coli promoters: the combined mode of action of Lac repressor and AraC activator. *Nucleic Acids Res*, **29**, 3873-3881.
26. Adamson, D.N. and Lim, H.N. (2011) Essential requirements for robust signaling in Hfq dependent small RNA networks. *PLoS Comput Biol*, **7**, e1002138.
37. Moon, K. and Gottesman, S. (2011) Competition among Hfq-binding small RNAs in Escherichia coli. *Mol Microbiol*, **82**, 1545-1562.
38. Altuvia, S., Weinstein-Fischer, D., Zhang, A., Postow, L. and Storz, G. (1997) A small, stable RNA induced by oxidative stress: role as a pleiotropic regulator and antimutator. *Cell*, **90**, 43-53.
43. Gotta, S.L., Miller, O.L., Jr. and French, S.L. (1991) rRNA transcription rate in Escherichia coli. *J Bacteriol*, **173**, 6647-6649.
53. Hopkins, J.F., Panja, S. and Woodson, S.A. (2011) Rapid binding and release of Hfq from ternary complexes during RNA annealing. *Nucleic Acids Res*, **39**, 5193-5202.
54. Repoila, F. and Gottesman, S. (2001) Signal transduction cascade for regulation of RpoS: temperature regulation of DsrA. *J Bacteriol*, **183**, 4012-4023.
55. Majdalani, N., Chen, S., Murrow, J., St John, K. and Gottesman, S. (2001) Regulation of RpoS by a novel small RNA: the characterization of RprA. *Mol Microbiol*, **39**, 1382-1394.
56. Pulvermacher, S.C., Stauffer, L.T. and Stauffer, G.V. (2009) Role of the Escherichia coli Hfq protein in GcvB regulation of oppA and dppA mRNAs. *Microbiology*, **155**, 115-123.
57. Moller, T., Franch, T., Hojrup, P., Keene, D.R., Bachinger, H.P., Brennan, R.G. and Valentin-Hansen, P. (2002) Hfq: a bacterial Sm-like protein that mediates RNA-RNA interaction. *Mol Cell*, **9**, 23-30.
58. Masse, E., Escorcia, F.E. and Gottesman, S. (2003) Coupled degradation of a small regulatory RNA and its mRNA targets in Escherichia coli. *Genes Dev*, **17**, 2374-2383.
59. Lacroute, F. and Stent, G.S. (1968) Peptide chain growth of -galactosidase in Escherichia coli. *J Mol Biol*, **35**, 165-173.
60. Young, R. and Bremer, H. (1976) Polypeptide-chain-elongation rate in Escherichia coli B/r as a function of growth rate. *Biochem J*, **160**, 185-194.

6. SUPPLEMENTARY FIGURE AND TABLE LEGENDS

Supplementary Figure S1. Comparison of the “basic” and “extended” models of sRNA regulation. **(A)** Figure showing the reaction steps in the extended model which explicitly includes Hfq and Hfq complexes. The rate constants are defined and their values specified in the section on the extended model in the **Supplementary Methods**. Degradation reactions are not shown. RNAP = RNA polymerase. **(B)** Comparison of the basic and extended models. The sRNA transcription rate is normalized to the target mRNA transcription rate ($1 \text{ nM}\cdot\text{min}^{-1}$) and a value of 1 (which is 0 on the \log_{10} scale) indicates they are equal (green vertical line). Over the regulatory range (yellow shaded area) the basic and extended models are comparable. **(C–E)** Target protein concentration in the extended model at different values for key parameters (note: in each plot only one parameter was altered compared to panel **B**). The basic model from panel B is reshown for comparison. Under some conditions there is less duplex formation in the extended model therefore the differences between the sRNA and TF response curves described in the main text and shown in **Figure 2** may be underestimated. **(C)** Extended model with Hfq production (α_H) increased or decreased by 10-fold. The Hfq concentration is important in the extended model with too little limiting the rate of duplex formation and too much resulting in sequestration of the sRNAs and target mRNAs which also limits duplex formation (26). **(D)** Extended model with no RNA dissociation from Hfq (*i.e.* k_{TS}^{-1} , k_T^{-1} , k_{STH}^{-1} and $k_{TSH}^{-1} = 0 \text{ min}^{-1}$). **(E)** Extended model with all the RNA association rate constants (k_S , k_T , k_{STH} and k_{TSH}) increased by 10-fold.

Supplementary Figure S2. GFP expression as a function of IPTG concentration measured *in vivo*. The *gfp* gene was placed directly under the control of the PLlacO-1 promoter (HL3190) to determine the relative level of transcription at different concentrations of IPTG. # corrected for background autofluorescence using a strain without GFP (HL716) (20). *Zero on the x-axis is the actual value not 10^0 .

Supplementary Figure S3. Representative histograms for the TF activator circuit (AraC-*ompC*, HL1289) at low ($0 \mu\text{M}$ IPTG), intermediate ($75 \mu\text{M}$ IPTG) and high ($1000 \mu\text{M}$ IPTG) transcription levels of *araC*. The distributions are unimodal at all levels of induction.

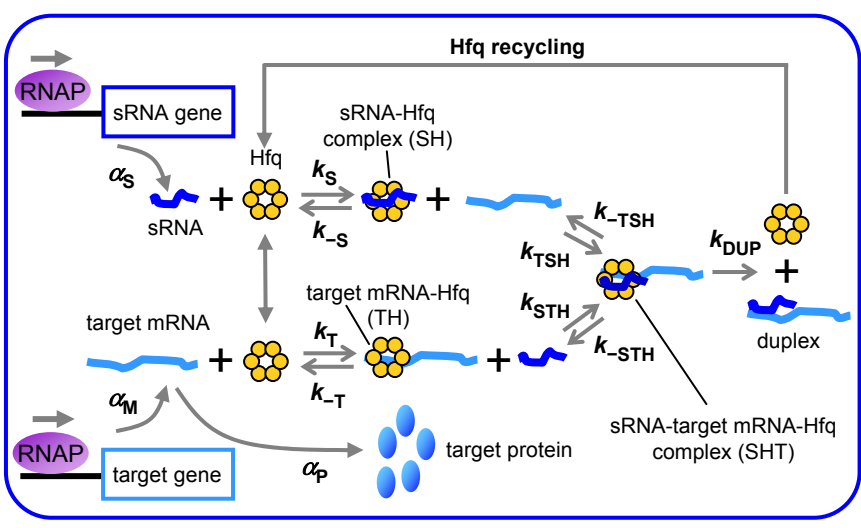
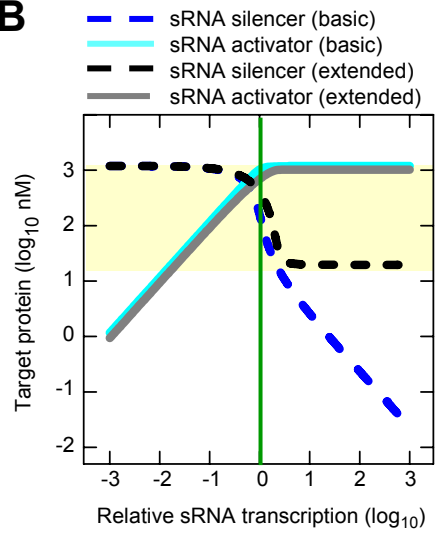
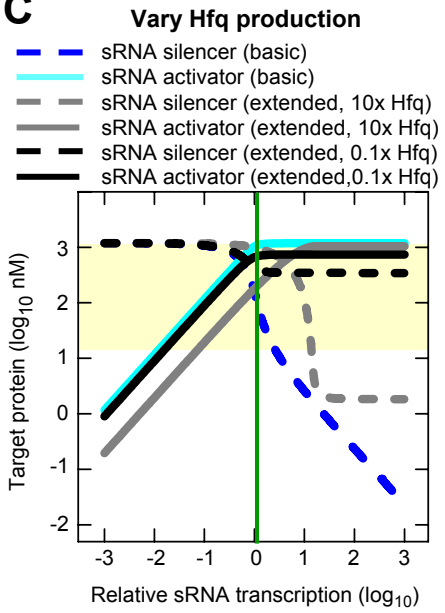
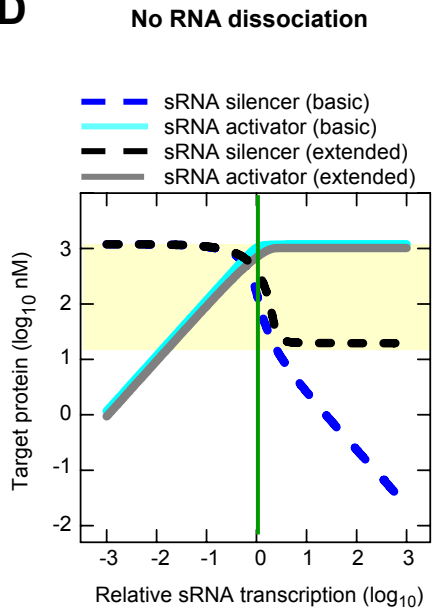
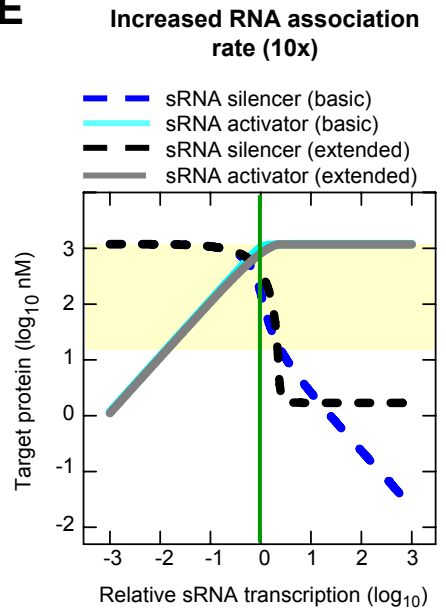
Supplementary Figure S4. Concentrations of sRNA and TF at different relative levels of sRNA and TF transcription. The relative transcription is the sRNA or TF transcription rate (α_S and α_{TFM} respectively) normalized to the target mRNA transcription ($\alpha_M = 1 \text{ nM}\cdot\text{min}^{-1}$). The green line indicates where the sRNA and target mRNA transcription are equal. To the left of the green line the free sRNA concentration is reduced due to duplex formation and to the right of the line there is insufficient target mRNA to form duplexes for all of the sRNAs transcribed.

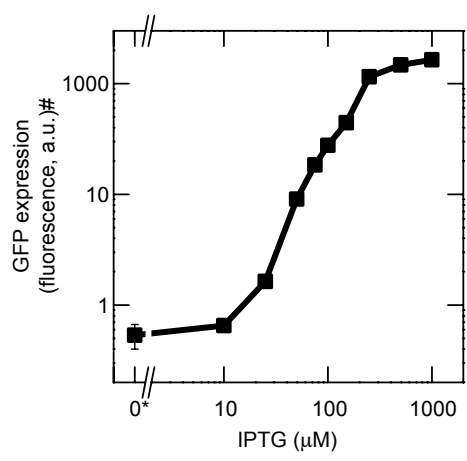
Supplementary Figure S5. sRNA silencing and sRNA activation with different sRNA half-lives. The simulation of the basic model shows the sRNA half-life has minimal impact on target expression levels. The values with the sRNA half-life of 5 min are the same as shown in **Figure 2C**.

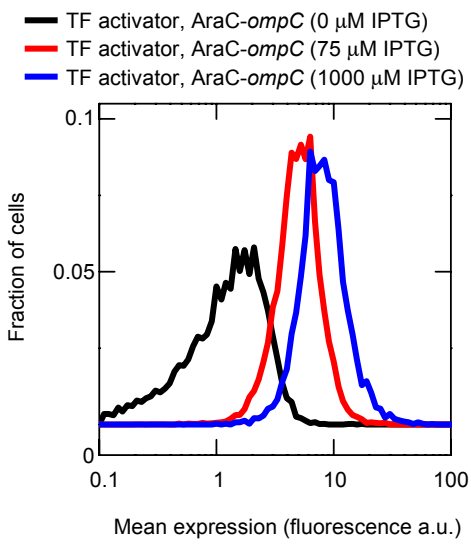
Supplementary Table S1. Strains. ‡ Previously described (20).

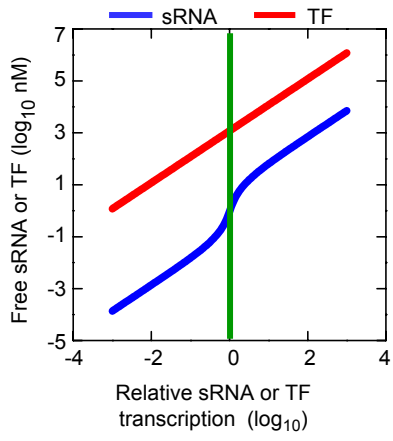
Supplementary Table S2. Plasmids. ‡ Previously described (20). ^ These plasmids have the same layout as pHL98 (20). ◇ These plasmids have the same layout as pHL404 (20) with *mCherry* replacing the sRNA, *araC* replacing *hfq*, or *Plar* replacing *PLtetO-1*.

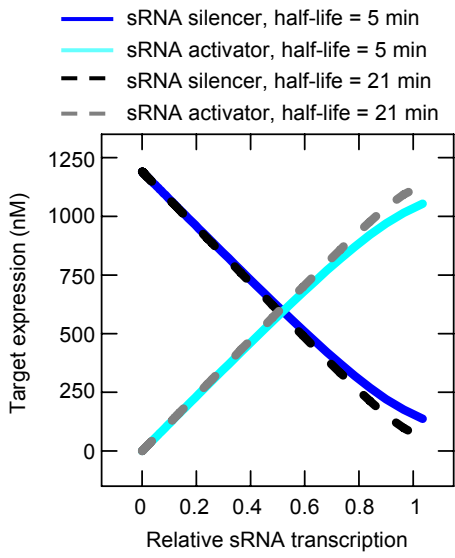
Supplementary Table S3. Oligonucleotides.

A**B****C****D****E**









Supplementary Table S1. Strains

Strain	Description
HL 862‡	HL 716 + $\Delta micC$
HL 865‡	HL 716 + $\Delta dsrA$
HL 1082	HL 862 + pHL 233
HL 1085	HL 862 + pHL 108
HL 1176	HL 862 + pHL 279
HL 1178‡	HL 862 + pHL 282
HL 1249	HL 862 + $\Delta araC$
HL 1286	HL 865 + $\Delta araC$
HL 1289	HL 1249 + pHL 342
HL 1299	HL 865 + pHL 98
HL 1449	HL 1286 + pHL 363
HL 3190	HL 716 + pHL 1023
HL 4870	HL 862 + pHL 1569
HL 4872	HL 862 + pHL 1571

Supplementary Table S2. Plasmids

Plasmid	Description
pHL 98‡	PLlacO-1: <i>dsrA-mCherry</i> , PLtetO-1: <i>rpoS::gfp</i>
pHL 108‡	PLlacO-1: <i>micC-mCherry</i> , PLtetO-1: <i>ompC::gfp</i>
pHL 233^	PLlacO-1: <i>tetR (st7)-mCherry</i> , PLtetO-1: <i>ompC::gfp</i>
pHL 279^	PLlacO-1: <i>tetR (st3)-mCherry</i> , PLtetO-1: <i>ompC::gfp</i>
pHL 282‡	PLtetO-1: <i>mCherry</i> , PLlacO-1: <i>ompC::gfp</i>
pHL 342◇	PLtetO-1: <i>mCherry</i> , PLlacO-1: <i>araC</i> , Plar: <i>ompC::gfp</i>
pHL 363◇	PLtetO-1: <i>dsrA</i> , PLlacO-1: <i>araC</i> , Plar: <i>rpoS::gfp</i>
pHL 1023^	PLtetO-1: <i>mCherry</i> , PLlacO-1: <i>gfp (st7)</i>
pHL 1569^	PLlacO-1: <i>micC-mCherry</i> , PLtetO-1: <i>ompC::gfp AAV tag</i>
pHL 1571^	PLlacO-1: <i>tetR (st3)-mCherry</i> , PLtetO-1: <i>ompC::gfp AAV tag</i>

Supplementary Table S3. Oligonucleotides

Oligonucleotide	Function	Sequence (5' to 3')
AraCRBSXmaKpnF	PCR amplify <i>araC</i> with RBS (st7)	cctcccgggtaaggaggaggtaccatggctgaagcgcaaaatgatcc
AraCApaR	PCR amplify <i>araC</i>	catgggccttatgacaactgacggctacat
AraCKOpkD1F	Delete chromosomal <i>araC</i>	tgcaatatggacaattggttctctctgaatgggtgggagatgaaaagtgtgaggctggagctgctc
AraCKOpkD4R	Delete chromosomal <i>araC</i>	caaaccctatgctactccgtcaagccgtcaattgtctgattcgttaccaaattcggggatccgtcgacc
AraCSeqUpF	Confirm deletion of <i>araC</i>	ttgggttagcgagaagagccagta
AraCDR	Confirm deletion of <i>araC</i>	cagcaatgcttgcataatgtgcct
GFPLVAshortR	First round PCR synthesis to add AAV tag to <i>gfp</i>	gcgtagtttctgctgttctgtctttgtatagttcatccatgccatg
AAVNheR	Second round PCR synthesis to add AAV tag to <i>gfp</i>	gccaagctagcattaaactgctgcagcgtagtttctgctgttctgctgc
TetRRBSXmalF	PCR amplify <i>tetR</i> with RBS (st7)	tcctccgggatcagcaggacgcactaaggaggaaaaaaatgtctagattagataaaagtaaag
TetRRBS3XmalF	PCR amplify <i>tetR</i> with RBS (st3)	tatccgggtaaggaggaaaatgtctagattagataaaagtaaag
TetRHindIIIR	PCR amplify <i>tetR</i>	ggccaagcttaagaccactttcacattaag